

Searches for Monojet and Monophoton Events with Missing Transverse Momentum with the ATLAS Detector

David Šálek
(CERN)

on behalf of the
ATLAS Collaboration

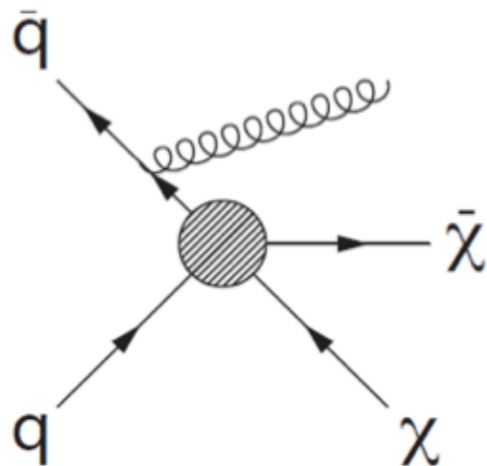
ICHEP2012
36th International Conference for High Energy Physics
Melbourne, 4 - 11 July 2012



Dark Matter Candidates

- Weakly Interacting Massive Particles (WIMPs)
 - They are expected to interact with SM particles via new couplings.
 - Assumptions:
 - WIMPs are produced in pairs at LHC.
 - Mediating particles between WIMPs and SM are too heavy to be produced directly.

➔ Effective field theory approach (contact interactions)



Name	Initial state	Type	Operator
D1	$q\bar{q}$	scalar	$\frac{m_q}{M_\star^3} \bar{\chi}\chi\bar{q}q$
D5	$q\bar{q}$	vector	$\frac{1}{M_\star^2} \bar{\chi}\gamma^\mu\chi\bar{q}\gamma_\mu q$
D8	$q\bar{q}$	axial-vector	$\frac{1}{M_\star^2} \bar{\chi}\gamma^\mu\gamma^5\chi\bar{q}\gamma_\mu\gamma^5 q$
D9	$q\bar{q}$	tensor	$\frac{1}{M_\star^2} \bar{\chi}\sigma^{\mu\nu}\chi\bar{q}\sigma_{\mu\nu} q$
D11	$g\bar{g}$	scalar	$\frac{1}{4M_\star^3} \bar{\chi}\chi\alpha_s(G_{\mu\nu}^a)^2$

- Detector signature is a jet or photon from initial state radiation (ISR) and missing transverse momentum (MET).

Large Extra Dimensions

- Models of large extra dimensions can provide an essential ingredient to a solution to the hierarchy problem.
- Arkani-Hamed, Dimopoulos, Dvali (ADD) model
 - Gravity propagates in (4+n)-dimensional bulk space.
 - Standard Model fields are confined to 4 dimensions.

$$M_{Pl}^2 \sim M_D^{2+n} R^n$$

M_{Pl} = 4-dimensional Planck scale

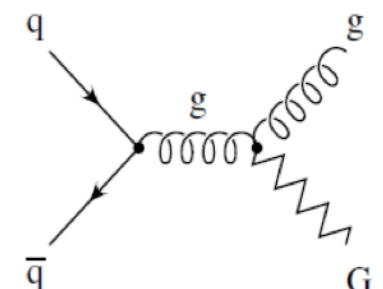
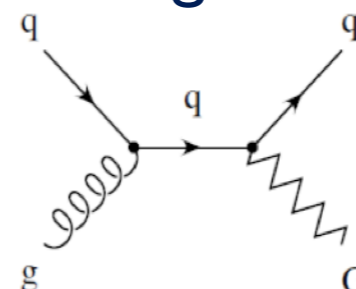
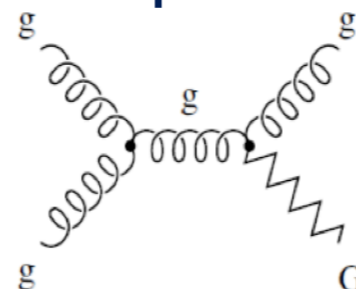
M_D = fundamental (4+n)-dimensional Planck scale

n = number of the extra dimensions

R = size of the extra dimensions

- The extra spatial dimensions are compactified resulting in Kaluza-Klein towers of massive graviton modes.
- At LHC, gravitons can be produced in association with jets or photons, leading to monojet or monophoton detector signatures.

$$\begin{aligned} qq &\rightarrow qG \\ gg &\rightarrow gG \\ q\bar{q} &\rightarrow gG, \gamma G \end{aligned}$$



Event Selection

● monojet selection

- all 2011 ATLAS pp data (4.7 fb^{-1})
- MET trigger (plateau above 150 GeV, 98% efficient at 120 GeV)
- primary vertex with at least 2 associated tracks
- leading jet $p_T > 120 \text{ GeV}$, $|\eta| < 2$
- $|\Delta\varphi(\text{jet2}, \text{MET})| > 0.5$
in order to suppress back-to-back dijet events
- no more than two jets with $p_T > 30 \text{ GeV}$, $|\eta| < 4.5$
- no electrons with $p_T > 20 \text{ GeV}$, $|\eta| < 2.47$
- no muons with $p_T > 7 \text{ GeV}$, $|\eta| < 2.5$
- signal regions with symmetric cuts on the leading jet p_T and MET
 $p_T, \text{MET} > 120, 220, 350, 500 \text{ GeV}$

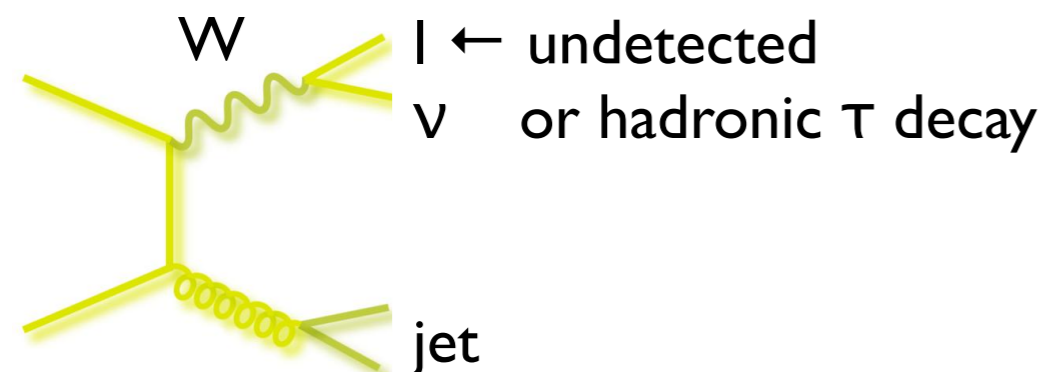
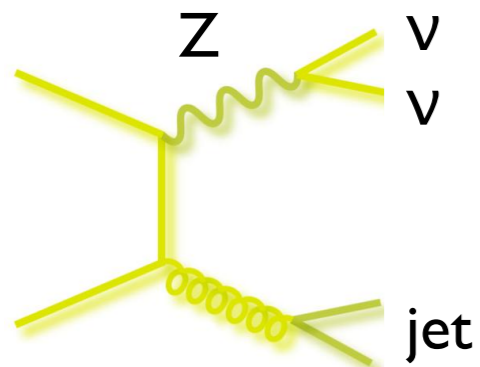
● monophoton selection

- all 2011 ATLAS pp data (4.6 fb^{-1}).
- MET trigger (98% efficient at 150 GeV)
- primary vertex with at least 5 associated tracks
- leading photon
 $p_T > 150 \text{ GeV}$, $|\eta| < 2.37$,
excluding calorimeter barrel/endcap transition region
 $1.37 < |\eta| < 1.52$
- overlap removal
 $|\Delta\varphi(\gamma, \text{MET})| > 0.4$,
 $|\Delta R(\text{jet}, \gamma)| > 0.4$,
 $|\Delta\varphi(\text{jet}, \text{MET})| > 0.4$
- no more than one jet with $p_T > 30 \text{ GeV}$, $|\eta| < 4.5$
- no electrons with $p_T > 20 \text{ GeV}$, $|\eta| < 2.47$
- no muons with $p_T > 10 \text{ GeV}$, $|\eta| < 2.5$

Background Estimation

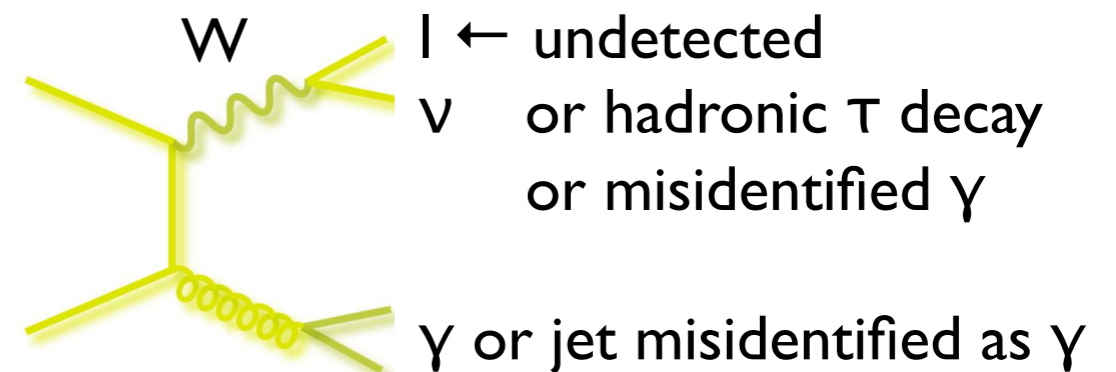
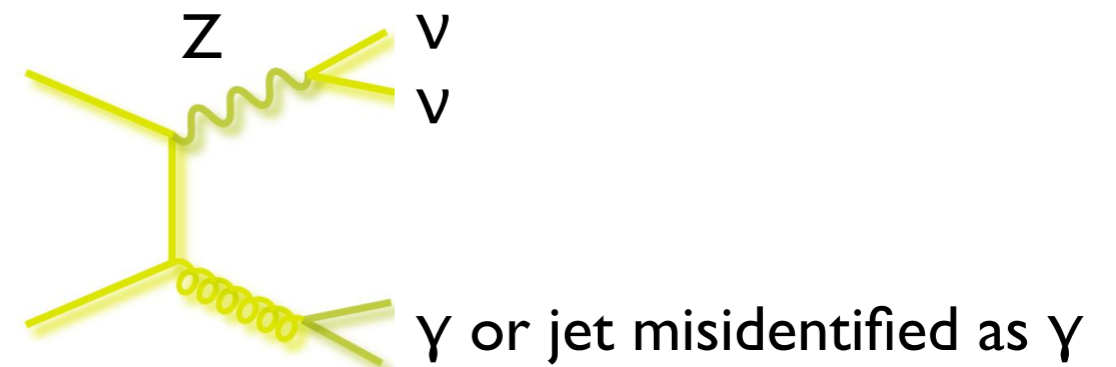
- **monojet analysis**

- electroweak backgrounds (estimated in data-driven way from control regions)
 - $Z \rightarrow \nu\nu + \text{jets}$
 - $W \rightarrow l\nu + \text{jets}$
 - $Z \rightarrow ll + \text{jets}$



- **monophoton analysis**

- electroweak backgrounds (estimated in data-driven way from control region)
 - $Z \rightarrow \nu\nu + \gamma$
 - $W \rightarrow l\nu + \gamma$
 - $Z \rightarrow ll + \gamma$
 - $W/Z + \text{jet}$



Background Estimation

● **monojet analysis**

- **electroweak backgrounds** (estimated in data-driven way from control regions)
 - $Z \rightarrow \nu\nu + \text{jets}$
 - $W \rightarrow l\nu + \text{jets}$
 - $Z \rightarrow ll + \text{jets}$
- **top quark production** (from MC)
- **multi-jet production** (from data)
 - di- or tri-jet events
- **non-collision backgrounds** (from data)
 - detector noise
 - cosmic ray showers
 - beam-induced background leading to fake jets
- **di-boson production** (from MC)
 - WW, WZ, ZZ

● **monophoton analysis**

- **electroweak backgrounds** (estimated in data-driven way from control region)
 - $Z \rightarrow \nu\nu + \gamma$
 - $W \rightarrow l\nu + \gamma$
 - $Z \rightarrow ll + \gamma$
 - $W/Z + \text{jet}$
- **$\gamma + \text{jet}$ and multi-jet production** (from data)
- **top quark production** (from MC)
- **$\gamma\gamma$ processes** (from MC)
- **di-boson production** (from MC)
- **non-collision backgrounds** (negligible)

Electroweak Backgrounds in the Monojet Analysis

- Data-driven estimation in four control regions (CR):

- $Z \rightarrow \mu\mu$
- $W \rightarrow \mu\nu$
- $Z \rightarrow ee$
- $W \rightarrow e\nu$

SR	$Z \rightarrow \nu\bar{\nu}+\text{jets}$	$W \rightarrow \tau\nu+\text{jets}$ $W \rightarrow \mu\nu+\text{jets}$	$W \rightarrow e\nu+\text{jets}$	$Z \rightarrow \tau^+\tau^-+\text{jets}$ $Z \rightarrow \mu^+\mu^-+\text{jets}$
CR	$W \rightarrow e\nu+\text{jets}$ $W \rightarrow \mu\nu+\text{jets}$ $Z \rightarrow e^+e^-+\text{jets}$ $Z \rightarrow \mu^+\mu^-+\text{jets}$	$W \rightarrow \mu\nu+\text{jets}$	$W \rightarrow e\nu+\text{jets}$	$Z \rightarrow \mu^+\mu^-+\text{jets}$

- Background is estimated in the following way:

$$N_{\text{SR}}^{\text{predicted}} = (N_{\text{CR}}^{\text{Data}} - N_{\text{Bkg}}) \cdot C \cdot \frac{N_{\text{SR}}^{\text{MC}}}{N_{\text{jet}/E_{\text{T}}^{\text{miss}}}^{\text{MC}}}$$

Electroweak Backgrounds in the Monojet Analysis

- Data-driven estimation in four control regions (CR):

- $Z \rightarrow \mu\mu$
- $W \rightarrow \mu\nu$
- $Z \rightarrow ee$
- $W \rightarrow e\nu$

SR	$Z \rightarrow \nu\bar{\nu}+\text{jets}$	$W \rightarrow \tau\nu+\text{jets}$ $W \rightarrow \mu\nu+\text{jets}$	$W \rightarrow e\nu+\text{jets}$	$Z \rightarrow \tau^+\tau^-+\text{jets}$ $Z \rightarrow \mu^+\mu^-+\text{jets}$
CR	$W \rightarrow e\nu+\text{jets}$ $W \rightarrow \mu\nu+\text{jets}$ $Z \rightarrow e^+e^-+\text{jets}$ $Z \rightarrow \mu^+\mu^-+\text{jets}$	$W \rightarrow \mu\nu+\text{jets}$	$W \rightarrow e\nu+\text{jets}$	$Z \rightarrow \mu^+\mu^-+\text{jets}$

- Background is estimated in the following way:

$$N_{\text{SR}}^{\text{predicted}} = (N_{\text{CR}}^{\text{Data}} - N_{\text{Bkg}}) \cdot C \cdot \frac{N_{\text{SR}}^{\text{MC}}}{N_{\text{jet}/E_{\text{T}}^{\text{miss}}}}^{\text{MC}}$$

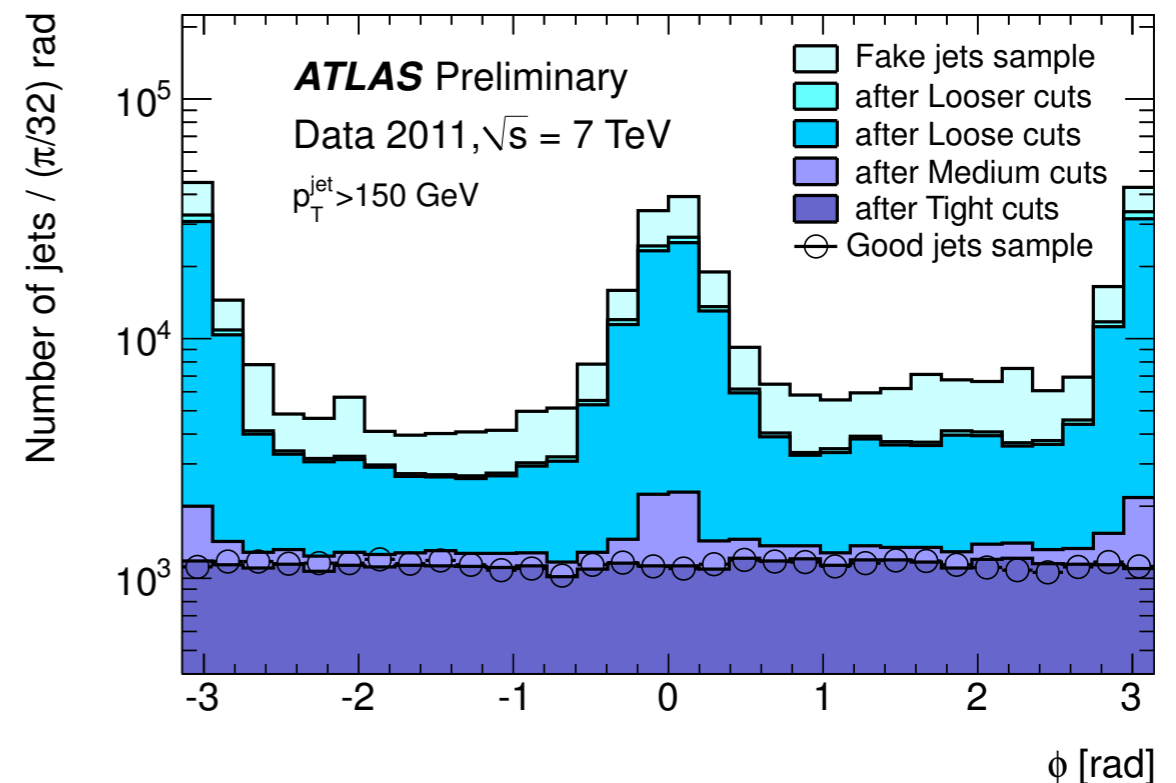
- The corrections are:

- multi-jet background in CR
- fraction of electroweak processes of a given kind in the control region
- lepton acceptance and reconstruction efficiency
- efficiency of the Z and W selection
- trigger efficiency and the luminosity correction (only for the electron CR)
- transfer factor from the full lepton phase space to the signal region (SR)

Non-Collision Backgrounds

- Beam background muons can deposit significant energy (up to $\sim \text{TeV}$) in the calorimeters that can be reconstructed as fake jets.
- Fake jets are balanced by MET.
 - Therefore, they lead to similar event topology as monojet signals.
 - They fire MET triggers.

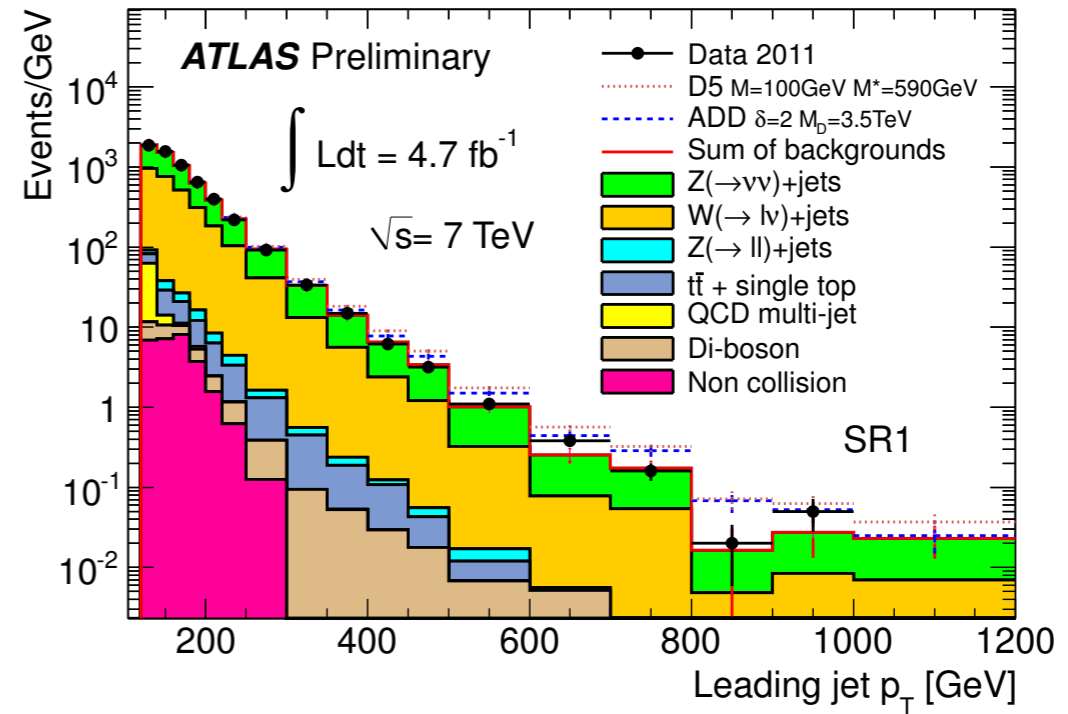
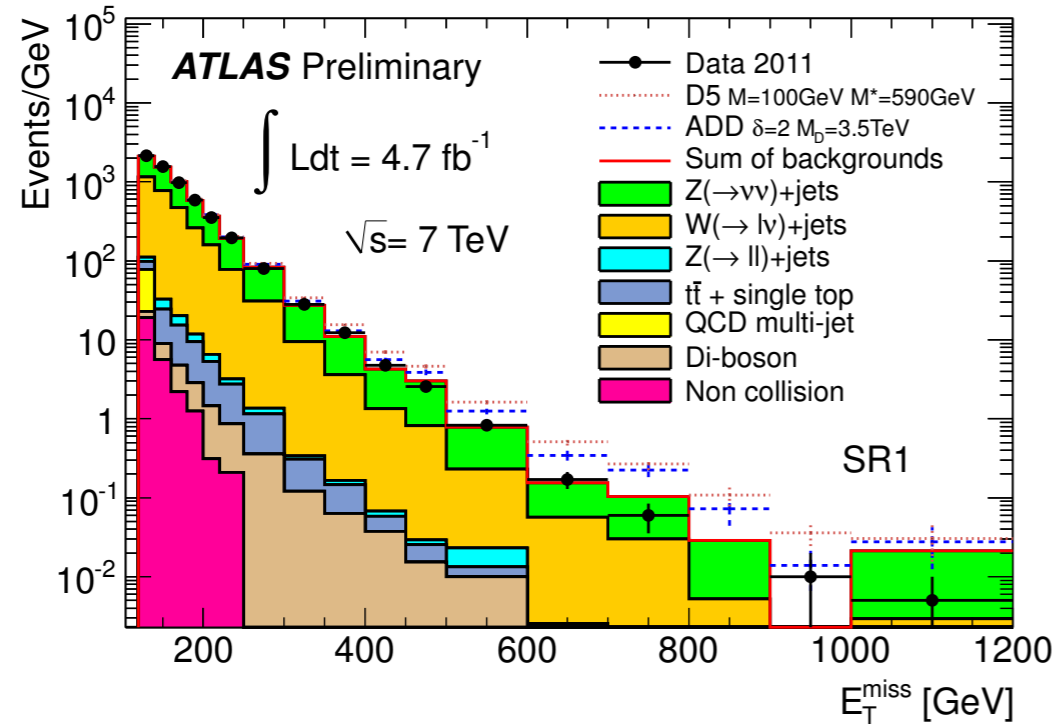
➔ Monojet analysis requires efficient fake jet removal.



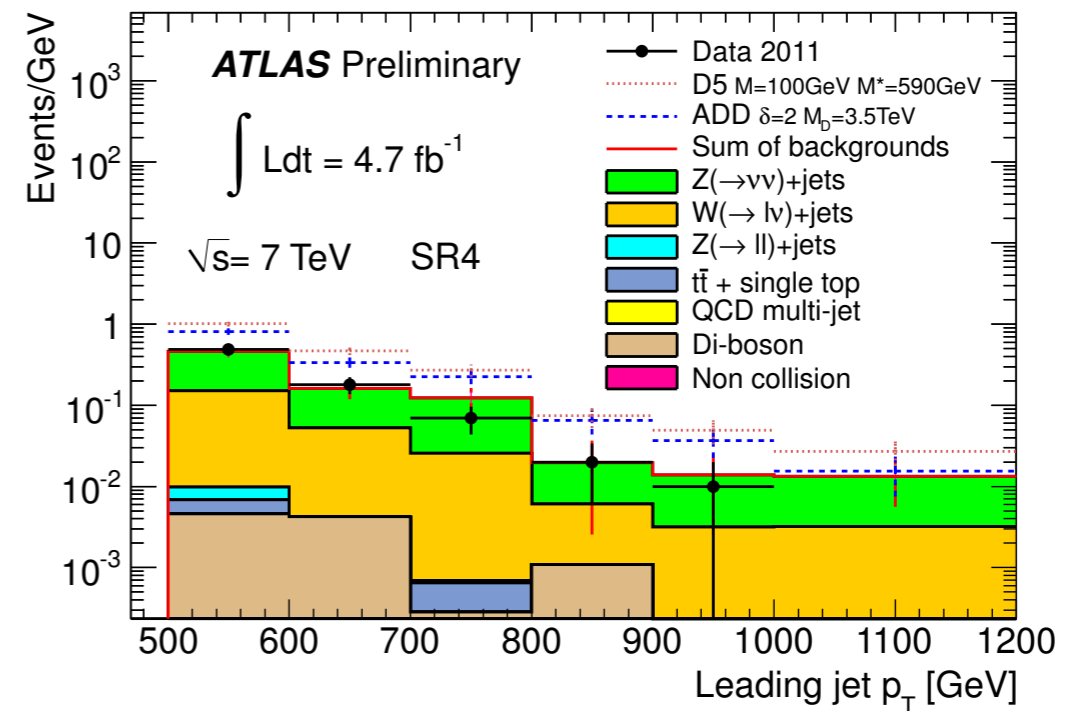
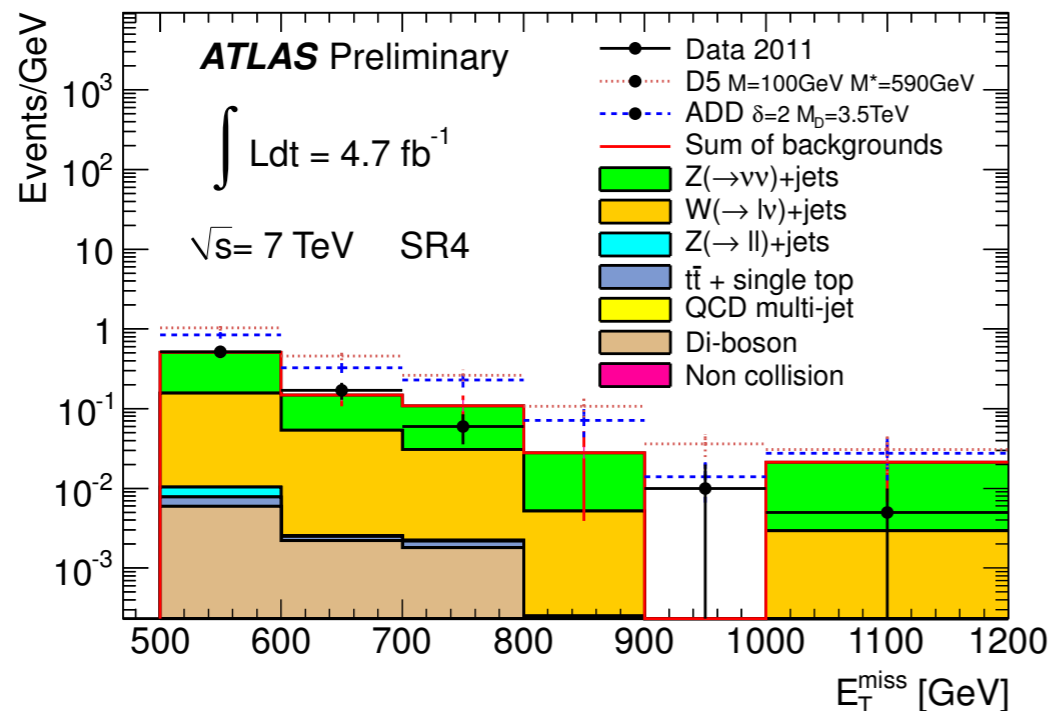
- Jet cleaning techniques based on jet quality criteria (e.g. jet charged fraction, electromagnetic fraction) provide efficient rejection at the level of 10^{-3} .
- Residual level of non-collision backgrounds is estimated with dedicated tool that searches for signatures of particles traversing the detector parallel to the beam pipe.

Monojet Results

- Signal region I



- Signal region 4



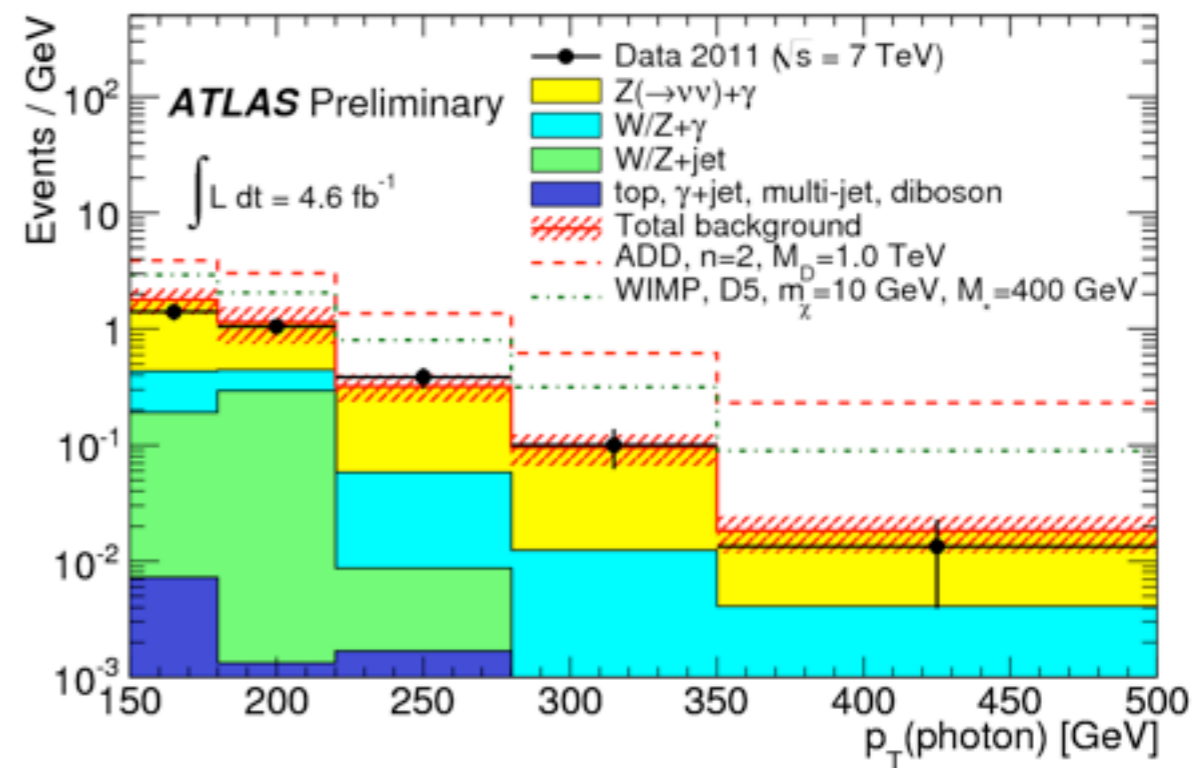
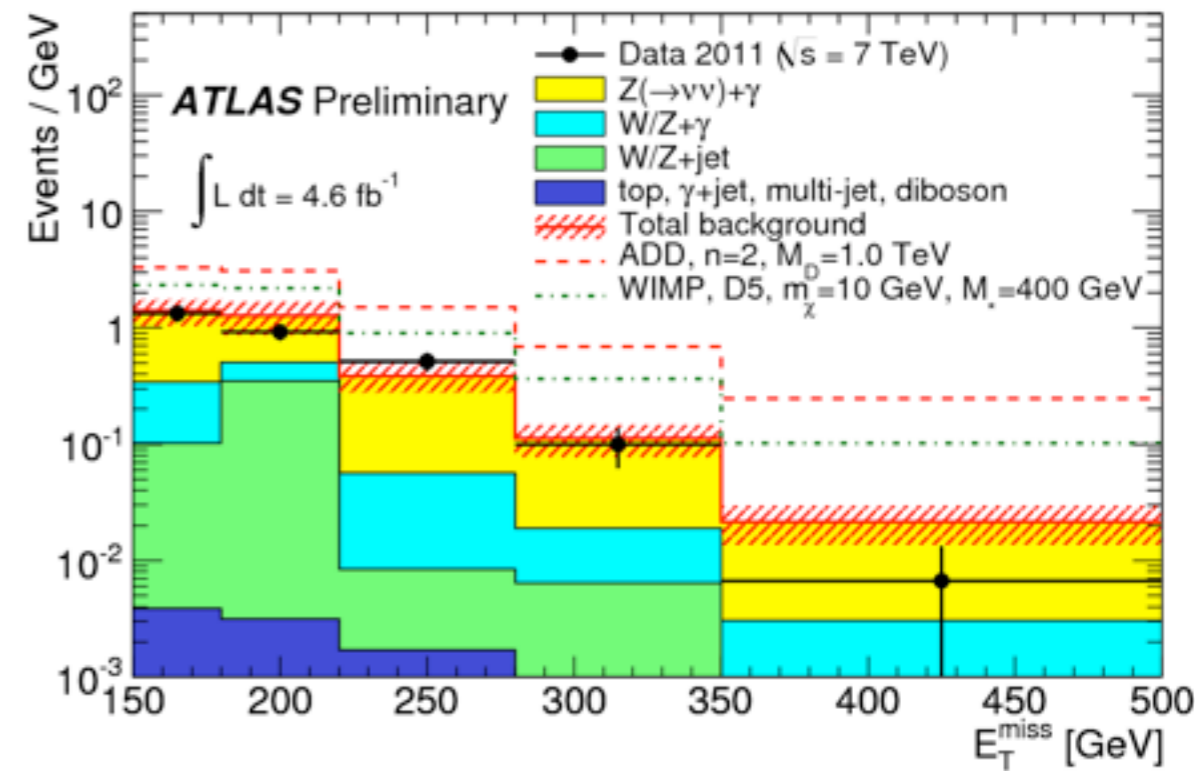
Monojet Results

	SR1	SR2	SR3	SR4
$Z \rightarrow \nu\bar{\nu}+\text{jets}$	63000 ± 2100	5300 ± 280	500 ± 40	58 ± 9
$W \rightarrow \tau\nu+\text{jets}$	31400 ± 1000	1853 ± 81	133 ± 13	13 ± 3
$W \rightarrow e\nu+\text{jets}$	14600 ± 500	679 ± 43	40 ± 8	5 ± 2
$W \rightarrow \mu\nu+\text{jets}$	11100 ± 600	704 ± 60	55 ± 6	6 ± 1
$t\bar{t} + \text{single } t$	1240 ± 250	57 ± 12	4 ± 1	-
Multijets	1100 ± 900	64 ± 64	8 ± 9	-
Non-coll. Background	575 ± 83	25 ± 13	-	-
$Z/\gamma^* \rightarrow \tau\tau+\text{jets}$	421 ± 25	15 ± 2	2 ± 1	-
Di-bosons	302 ± 61	29 ± 5	5 ± 1	1 ± 1
$Z/\gamma^* \rightarrow \mu\mu+\text{jets}$	204 ± 19	8 ± 4	-	-
Total Background	124000 ± 4000	8800 ± 400	748 ± 60	83 ± 14
Events in Data (4.7fb^{-1})	124703	8631	785	77

- Four independent determinations of $Z \rightarrow \nu\nu + \text{jets}$, based on the four control regions, are combined.
 - Background estimates are consistent with the number of observed events in all signal regions.
- ➡ 90% and 95% confidence level upper limits on the visible cross section ($\sigma \times A \times \epsilon$) are set.

Monophoton Results

Background source	Prediction	\pm (stat.)	\pm (syst.)
$Z(\rightarrow \nu\nu) + \gamma$	93	± 16	± 8
$Z/\gamma^*(\rightarrow \ell^+\ell^-) + \gamma$	0.4	± 0.2	± 0.1
$W(\rightarrow \ell\nu) + \gamma$	24	± 5	± 2
$W/Z + \text{jets}$	18	–	± 6
top	0.07	± 0.07	± 0.01
$WW, WZ, ZZ, \gamma\gamma$	0.3	± 0.1	± 0.1
γ +jets and multi-jet	1.0	–	± 0.5
Non-collision background	–	–	–
Total background	137	± 18	± 9
Events in data (4.6 fb^{-1})	116		

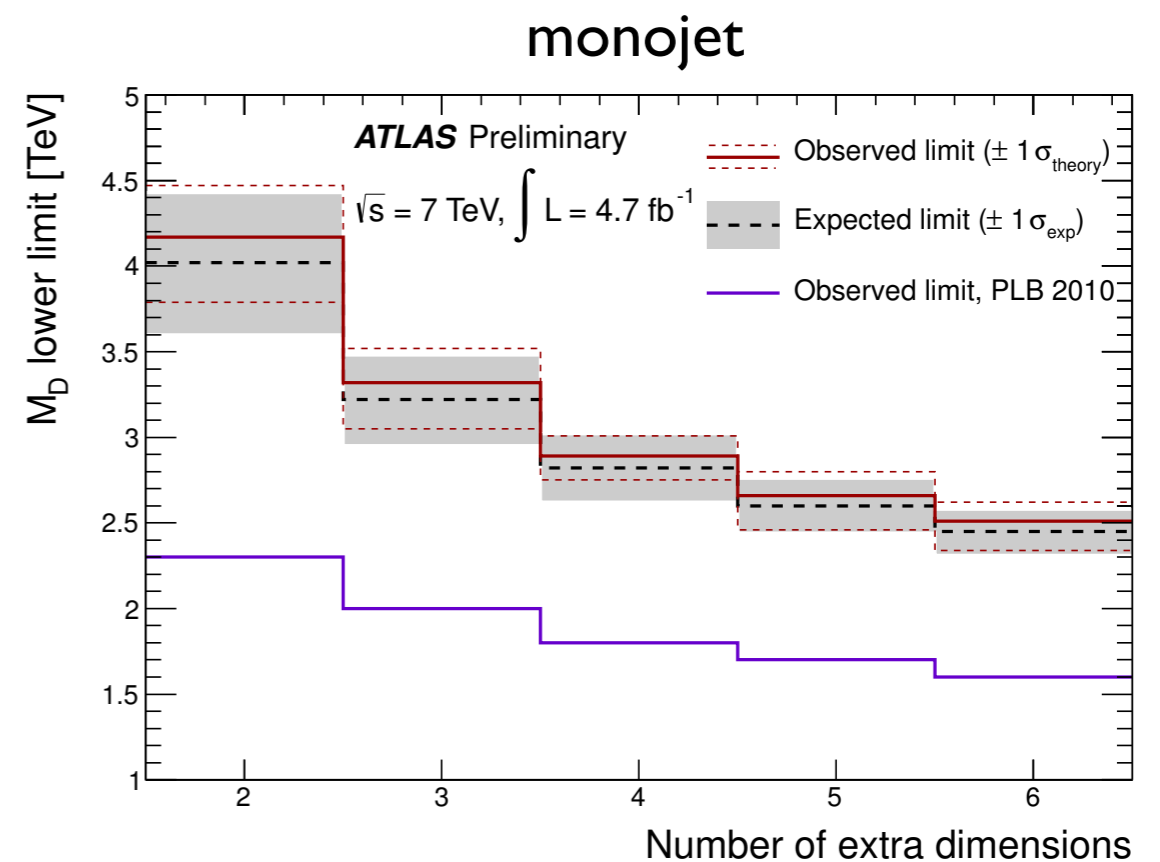
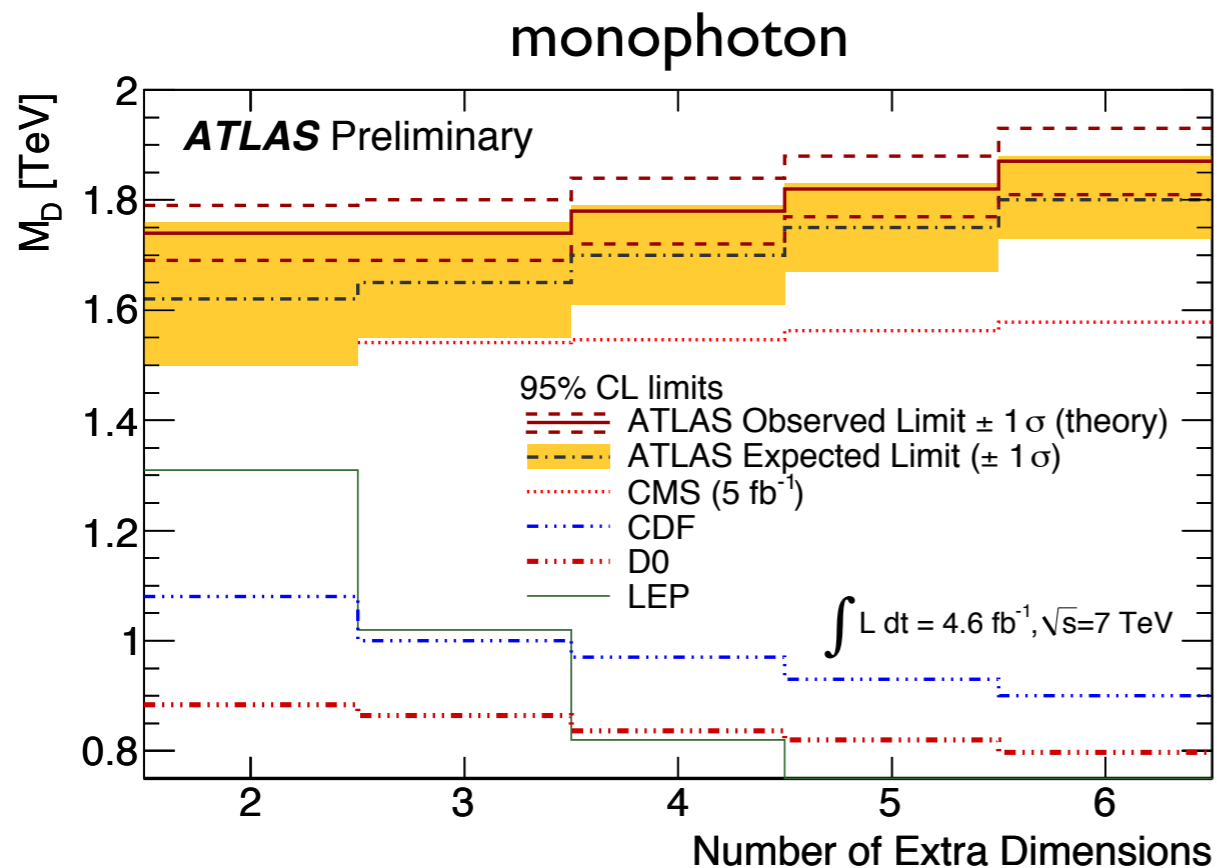


- Background estimates are consistent with the number of observed events in the signal region.

➡ 90% and 95% confidence level upper limits on the visible cross section ($\sigma \times A \times \epsilon$) are set.

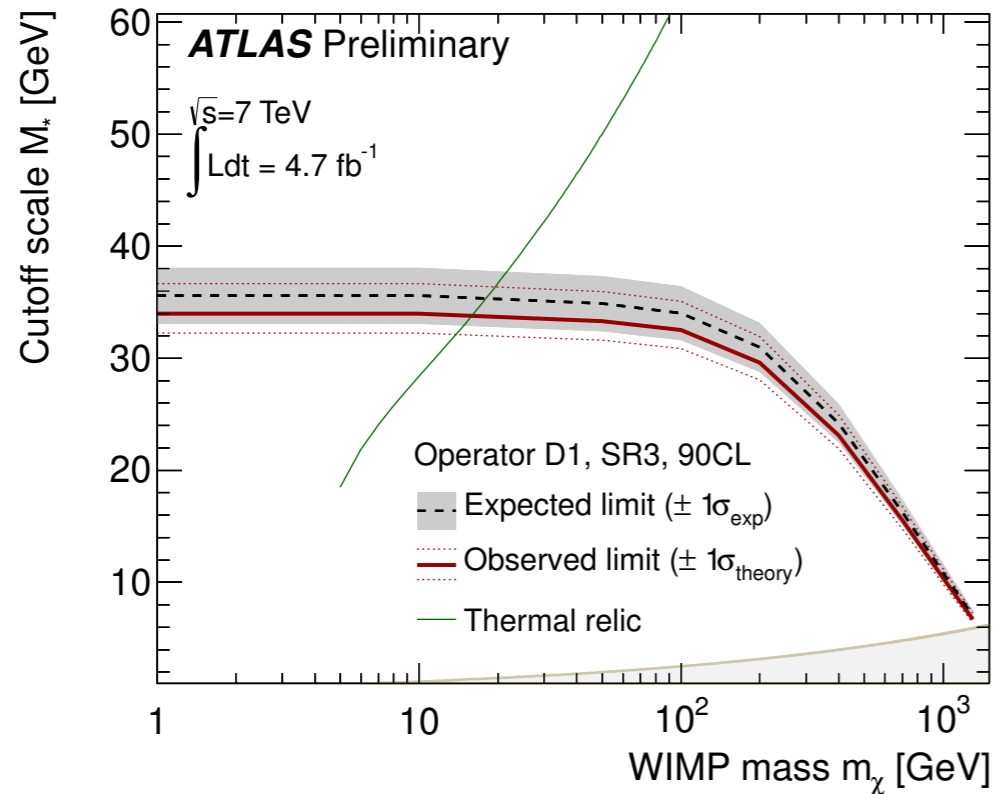
ADD Limits

- Theoretical uncertainties on ADD are associated with PDF uncertainties, ISR/FSR, factorization and renormalization scales.
- 95% CL limits on M_D as a function of the number of extra dimensions are set.



- ➔ M_D values below 1.74 TeV ($n=2$) and 1.87 TeV ($n=6$) are excluded (monophoton).
- ➔ M_D values below 3.79 TeV ($n=2$) and 2.34 TeV ($n=6$) are excluded (monojet).

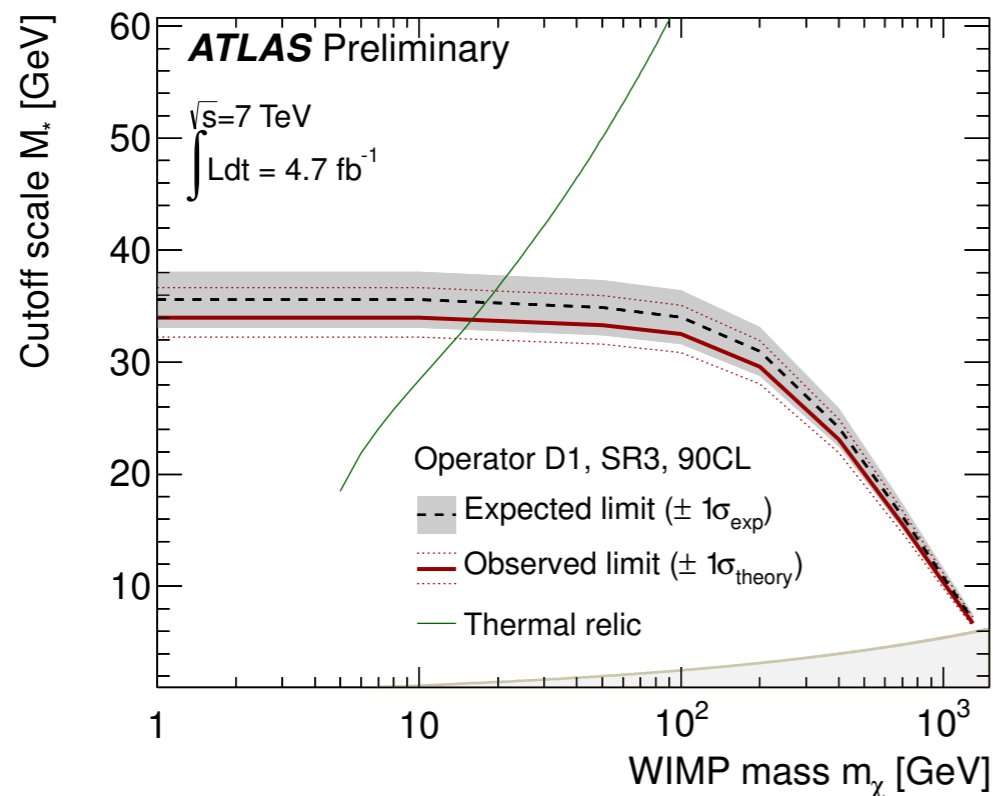
Limits on WIMP mass



Name	Initial state	Type	Operator
D1	qq	scalar	$\frac{m_q}{M_\star^3} \bar{\chi} \chi \bar{q} q$
D5	qq	vector	$\frac{1}{M_\star^2} \bar{\chi} \gamma^\mu \chi \bar{q} \gamma_\mu q$
D8	qq	axial-vector	$\frac{1}{M_\star^2} \bar{\chi} \gamma^\mu \gamma^5 \chi \bar{q} \gamma_\mu \gamma^5 q$
D9	qq	tensor	$\frac{1}{M_\star^2} \bar{\chi} \sigma^{\mu\nu} \chi \bar{q} \sigma_{\mu\nu} q$
D11	gg	scalar	$\frac{1}{4M_\star^3} \bar{\chi} \chi \alpha_s (G_{\mu\nu}^a)^2$

- Lower limits at 90% CL on the suppression scale M_\star are set for different operators as a function of WIMP mass m_χ .
- SR3 is used for D1, D5 and SR4 is used for D9, D11.

Limits on WIMP mass

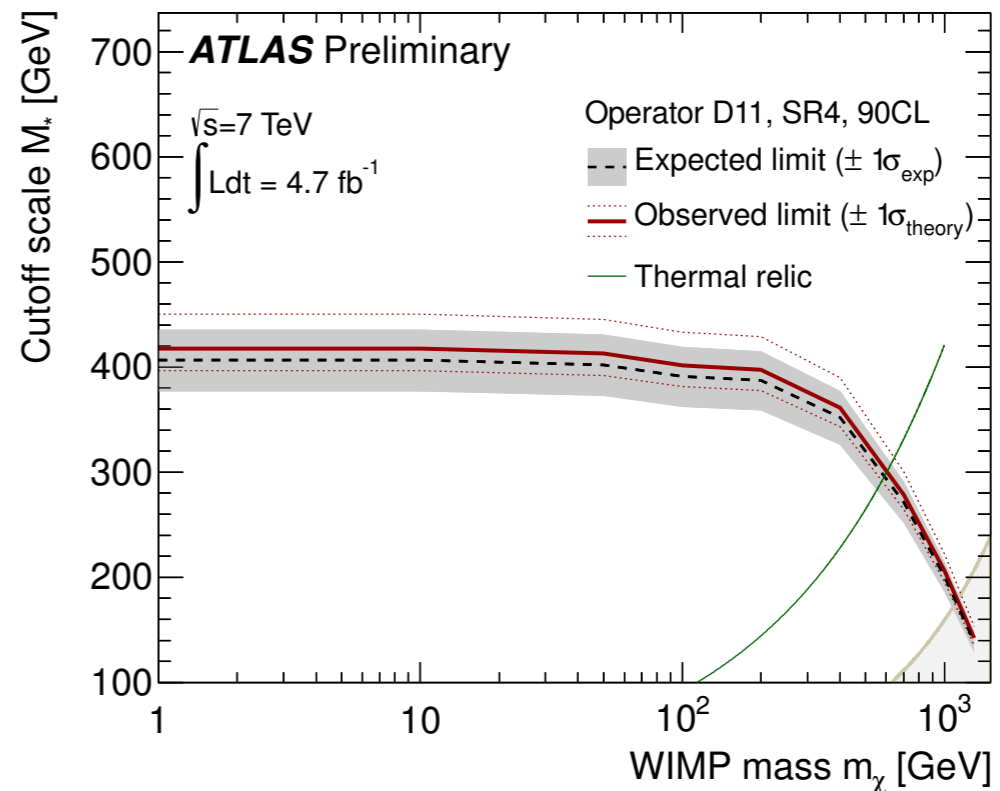
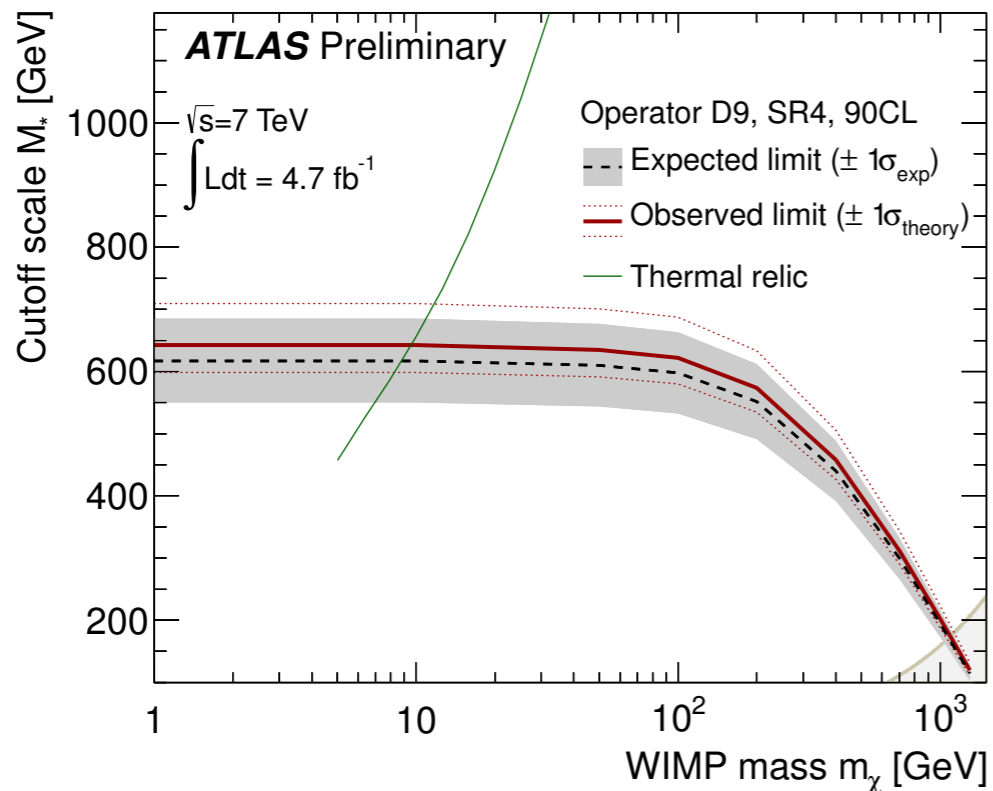
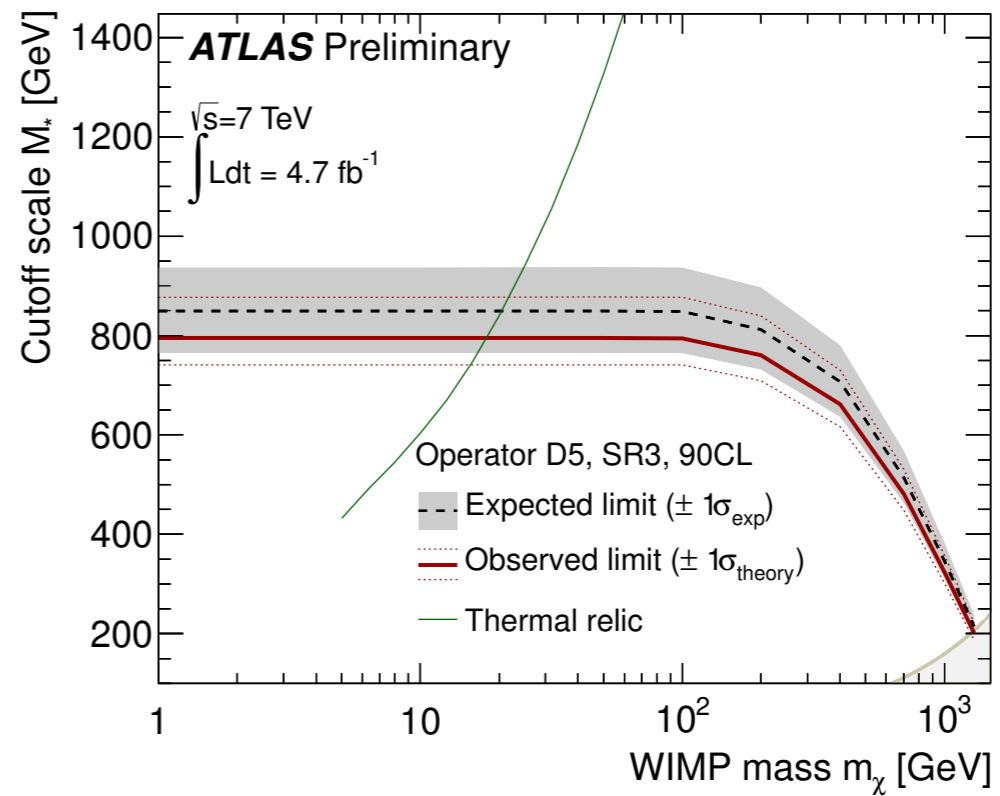
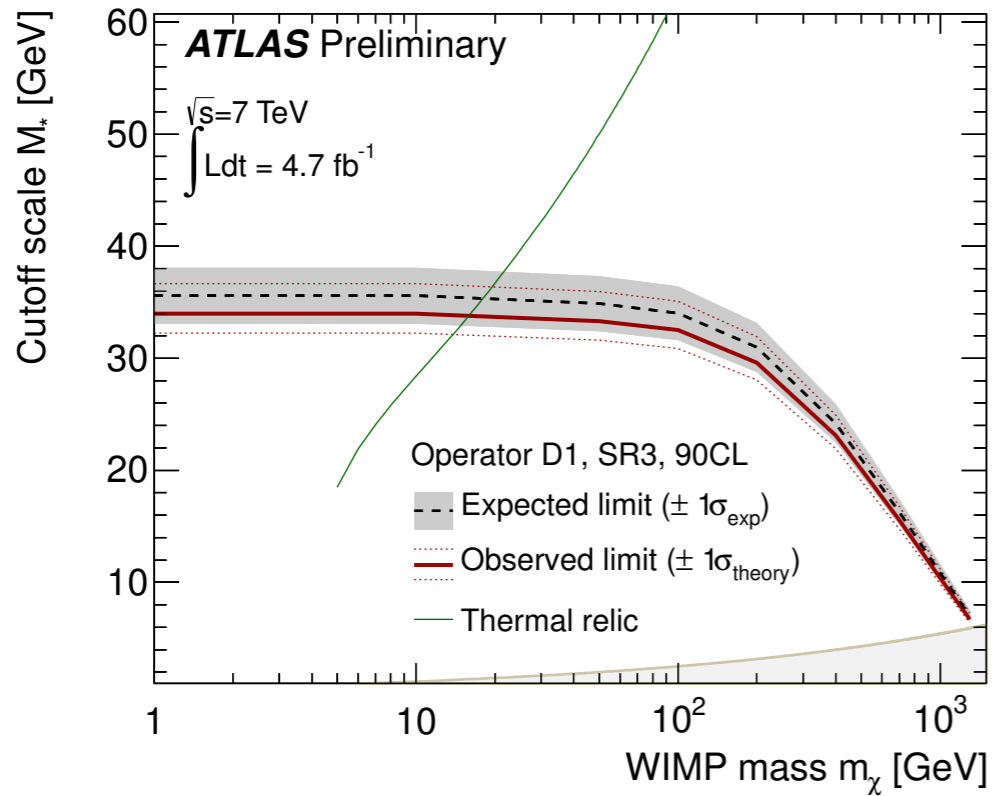


$$\Omega_X \propto \frac{1}{\langle \sigma v \rangle} \sim \frac{m_X^2}{g_X^4}$$

- Ω_X observed thermal relic density ≈ 0.24
- $\langle \sigma v \rangle$ thermally-averaged annihilation cross section
- m_X WIMP mass
- g_X WIMP coupling

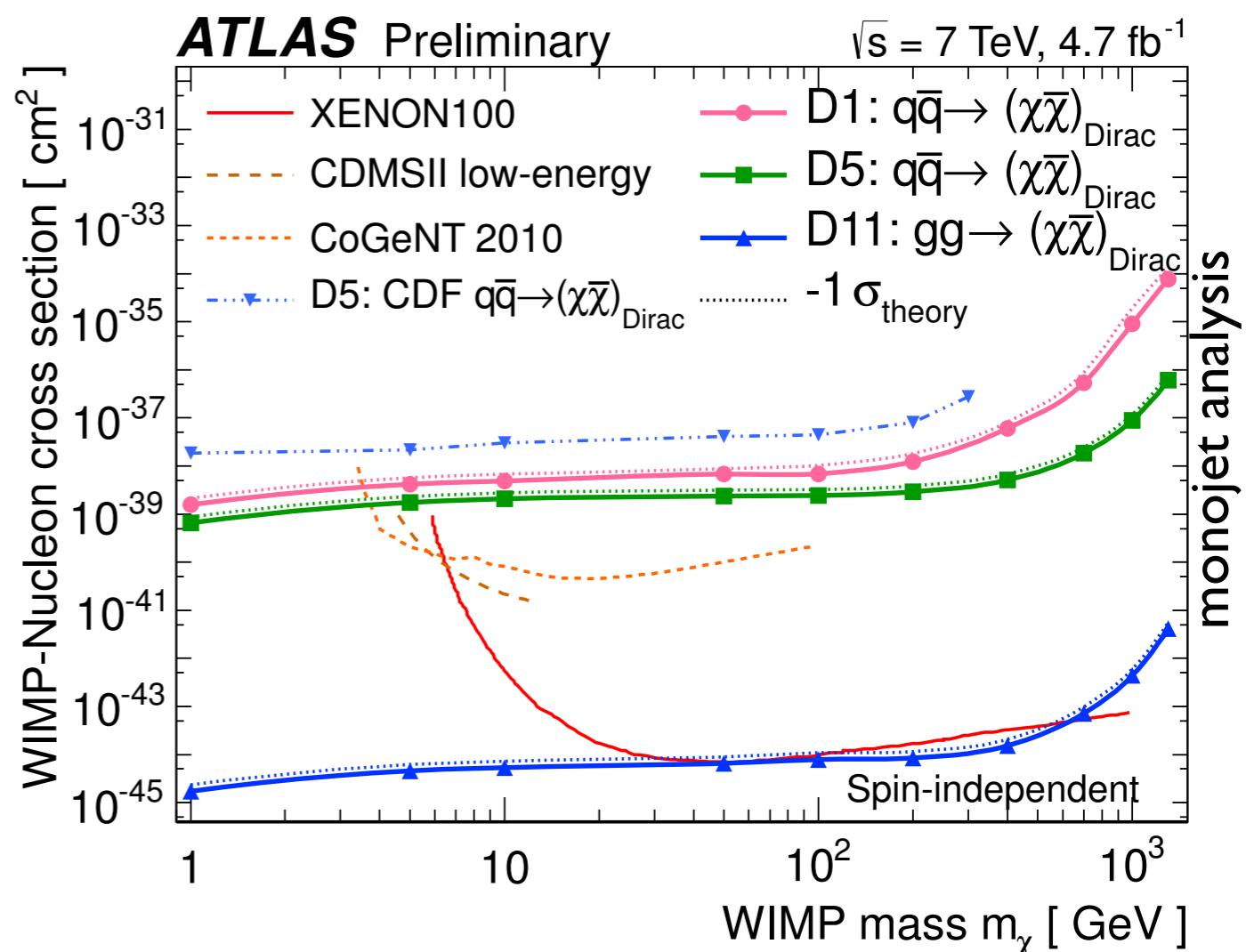
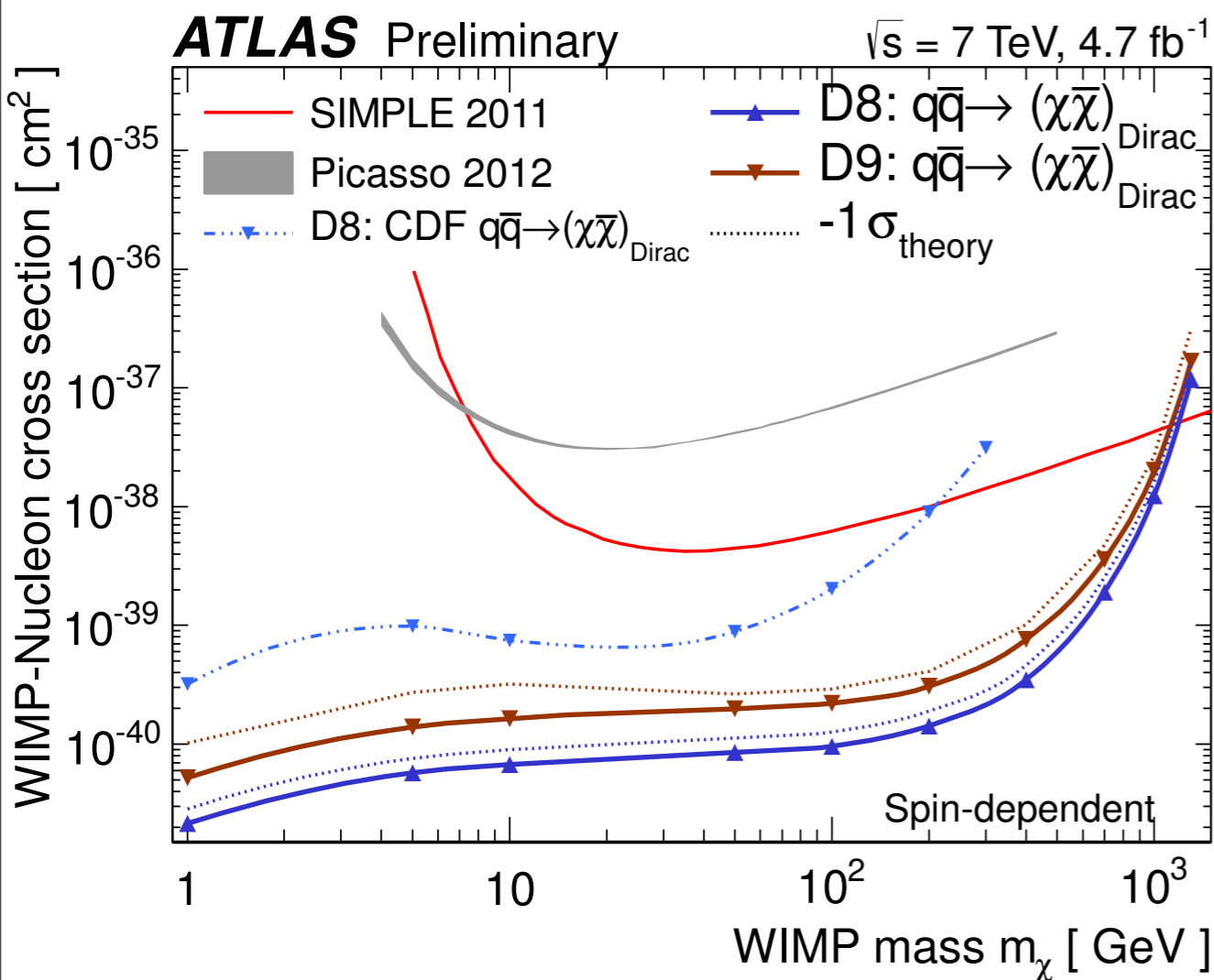
- **WIMP miracle:** The observed thermal relic density can be due to dark matter if the mass and the coupling of WIMPs is comparable to weak scale masses and weak force.
 $(m_X, g_X) \sim (m_{\text{weak}}, g_{\text{weak}})$
- ➔ Thermal relic density based on WMAP measurements is also indicated assuming that WIMPs annihilate exclusively via a particular operator to four light SM quarks.
- ➔ Above the thermal relic line, other couplings must exist if the WIMP miracle is still true.

Limits on WIMP mass



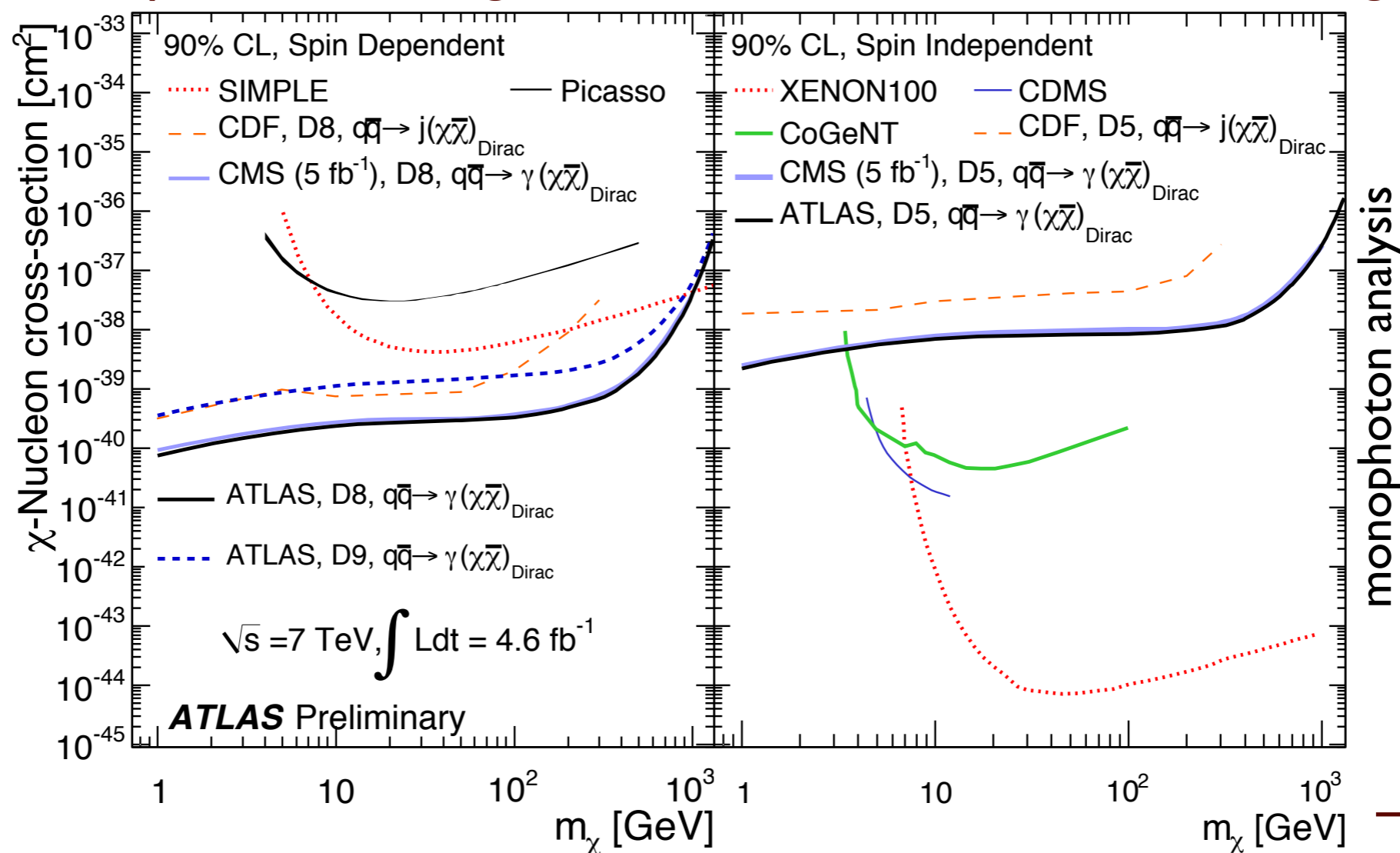
WIMP-nucleon scattering cross section limits

- Bounds on M_* can be converted to bounds on WIMP-nucleon scattering in the effective operator approach.
- ➔ comparison with direct dark matter detection experiments
 - spin-dependent (SIMPLE, Picasso)
 - ATLAS provides stronger limits for D8 (axial-vector) and D9.
 - spin-independent (XENON100, CDMSII, CoGeNT)
 - ATLAS provides stronger limits for D1 and D5 at low m_χ region.



WIMP-nucleon scattering cross section limits

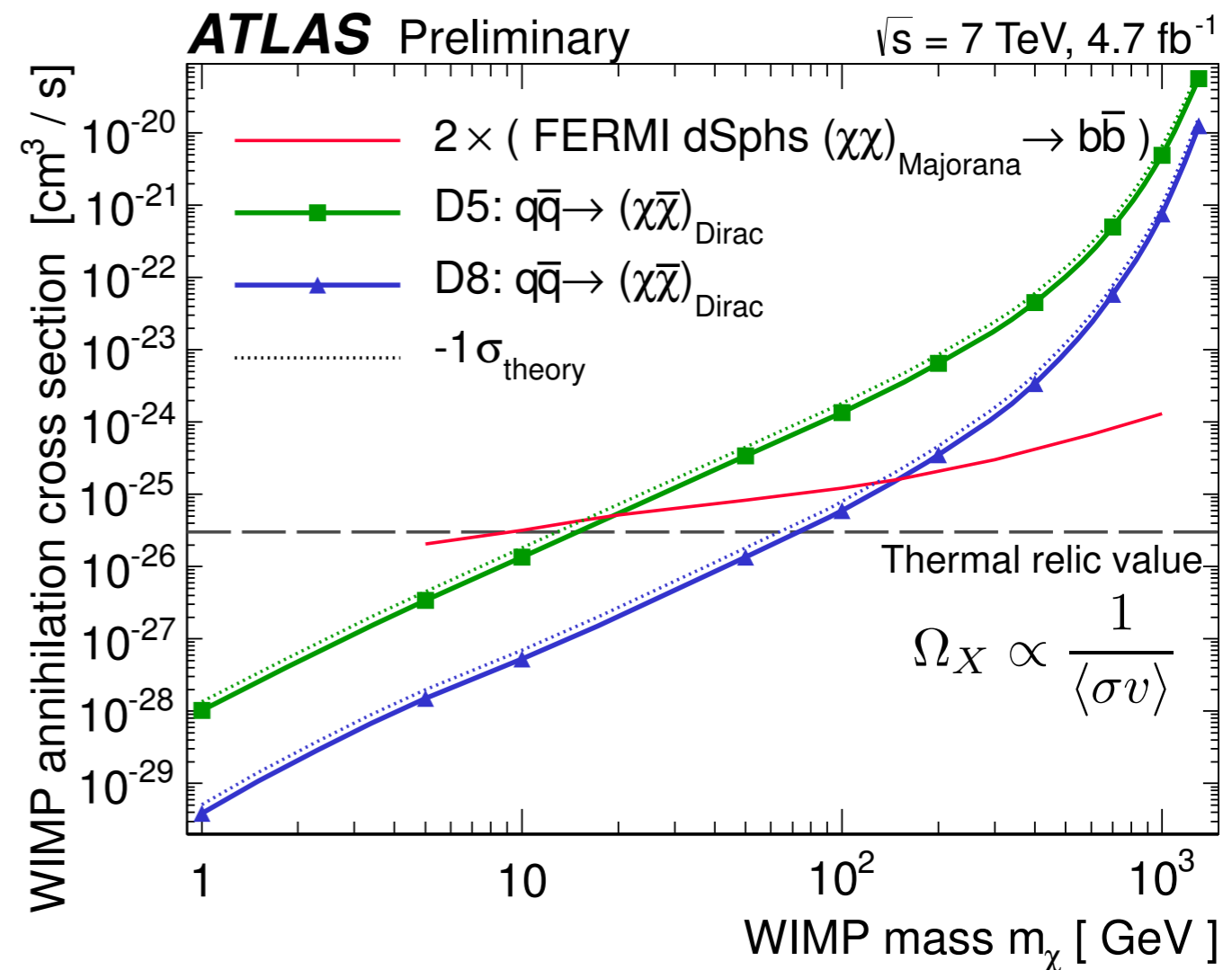
- Bounds on M_* can be converted to bounds on WIMP-nucleon scattering in the effective operator approach.
- ➔ comparison with direct dark matter detection experiments
 - spin-dependent (SIMPLE, Picasso)
 - ATLAS provides stronger limits for D8 (axial-vector) and D9.
 - spin-independent (XENON100, CDMSII, CoGeNT)
 - ATLAS provides stronger limits for D1 and D5 at low m_χ region.



Relic abundance of WIMPs

- The limits on vector and axial-vector interactions can be translated into cross section upper limits on WIMP annihilations into the four light quark flavors, assuming the interactions are flavor universal.
- The results are compared to the annihilations to $b\bar{b}$ from Galactic high energy gamma ray observations by FERMI LAT.

- ➔ The results are comparable and complementary.
- ➔ Below 10 GeV for D5 and 70 GeV for D8, the ATLAS limits are below the values needed for WIMPs to make up the cold dark matter abundance in the early universe (provided WIMPs annihilate exclusively via a particular operator).
- ➔ Above the thermal relic line, the abundance is too large and other operators are needed.



Summary

- Searches for physics beyond Standard Model in events with monojet and monophoton signatures are carried out with the full 2011 pp dataset.
ATLAS-CONF-2012-084, ATLAS-CONF-2012-085
- Four signal regions in the monojet analysis and one in the monophoton analysis (symmetric in the leading jet p_T and MET lower boundaries) are defined.
- In each region, data agree with the Standard Model predictions.
- Limits on the visible cross section of any Beyond Standard Model signal are set.
- Extra large dimensions (ADD model)
 - Lower limits are set on the $(4+n)$ -dimensional Planck scale M_D for different numbers of extra dimensions n .
- WIMP pair production
 - Effective field theory is used to derive limits on a mass suppression scale M_* .
 - The results are converted into limits on WIMP-nucleon scattering and WIMP annihilation cross sections and compared with direct dark matter detection experiments.
 - ATLAS provides complementary results to the direct WIMP searches.

backup

Limits on the visible cross section ($\sigma \times A \times \epsilon$)

- monojet analysis

	SR1	SR2	SR3	SR4
$\sigma_{\text{vis}}^{\text{obs}}$ at 90% [pb]	1.63	0.13	0.026	0.006
$\sigma_{\text{vis}}^{\text{exp}}$ at 90% [pb]	1.54	0.15	0.020	0.006
$\sigma_{\text{vis}}^{\text{obs}}$ at 95% [pb]	1.92	0.16	0.030	0.007
$\sigma_{\text{vis}}^{\text{exp}}$ at 95% [pb]	1.82	0.17	0.024	0.008

- monophoton analysis

- 90% CL upper limit = 5.6 fb
- 95% CL upper limit = 6.8 fb

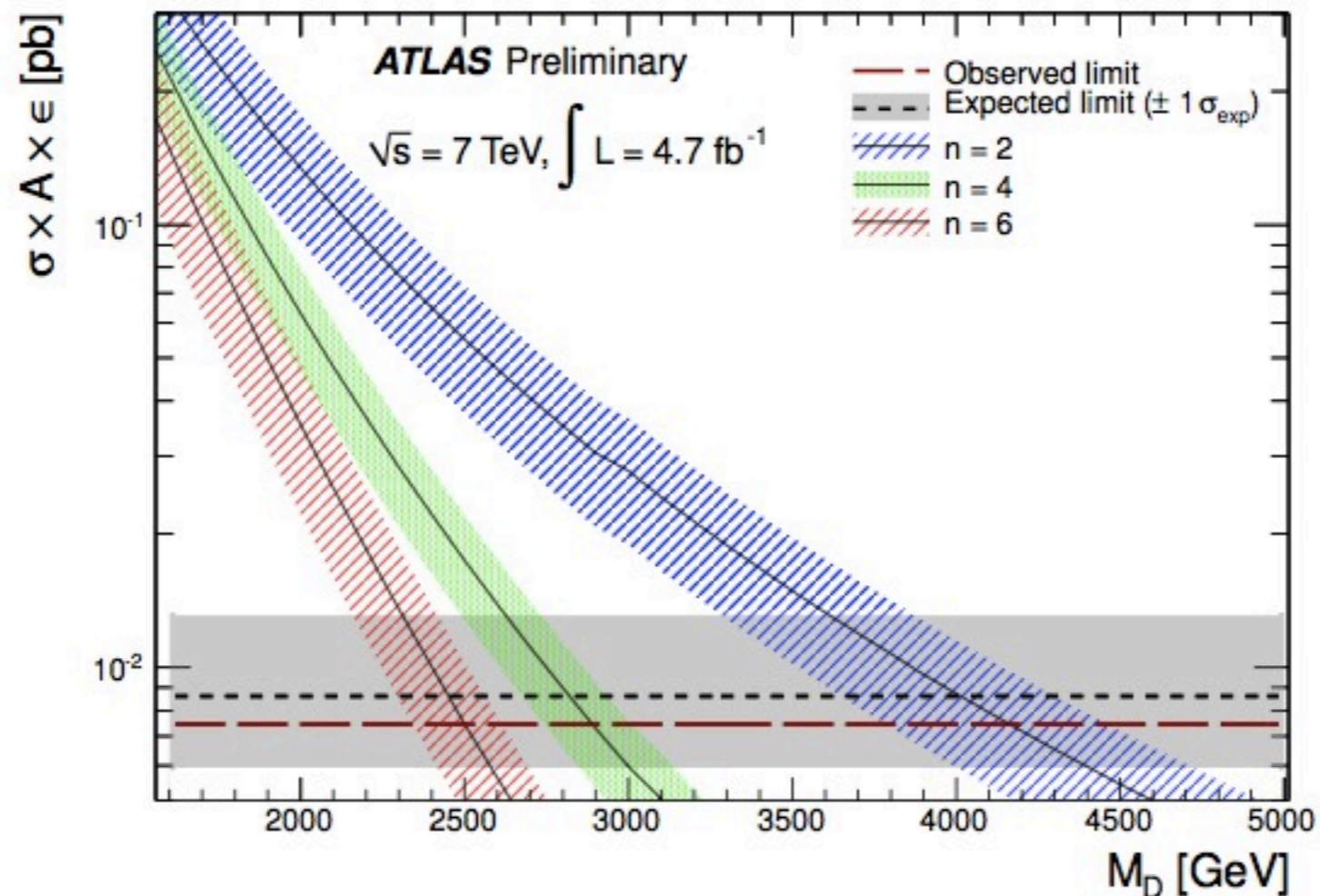
ADD limits in the monojet analysis

- The limits on ADD are extracted using the full simulated phase space.
- However, the effective field-theory is valid only for $\sqrt{s} < M_D$.
- The difference between the full cross sections and the ones truncated to the region of validity of the effective theory is between 6% and 60% depending on the number of extra dimensions.

n	M_D [TeV]	R [pm]	Cross section truncation [%]
2	3.79	3.3×10^7	0.2
3	3.05	5.6×10^2	5.9
4	2.75	2.1	19.9
5	2.46	8.0×10^{-2}	45.1
6	2.34	0.9×10^{-2}	63.4

ADD limits on the visible cross sections in the monojet analysis

- 95% CL limits on the visible cross sections ($\sigma \times A \times \epsilon$) at LO are obtained from SR4 for 2 - 6 extra dimensions.

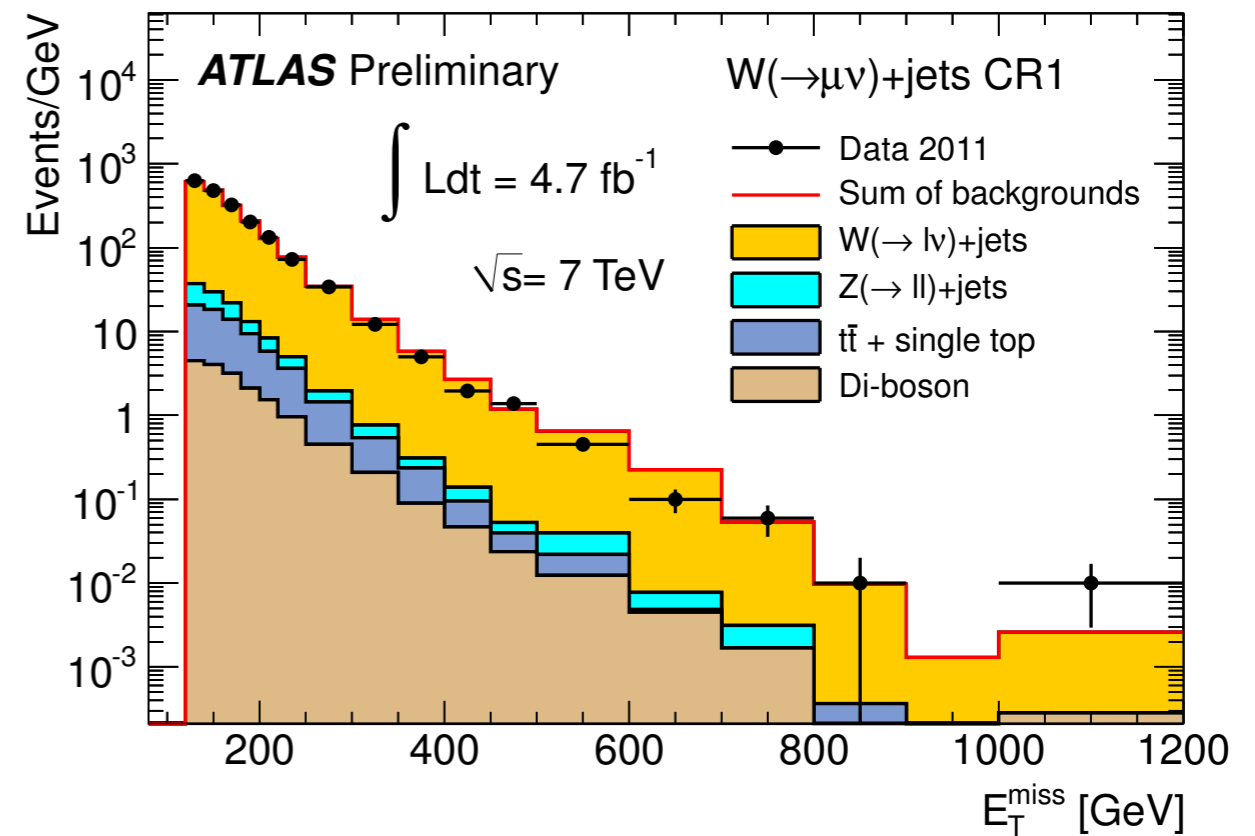
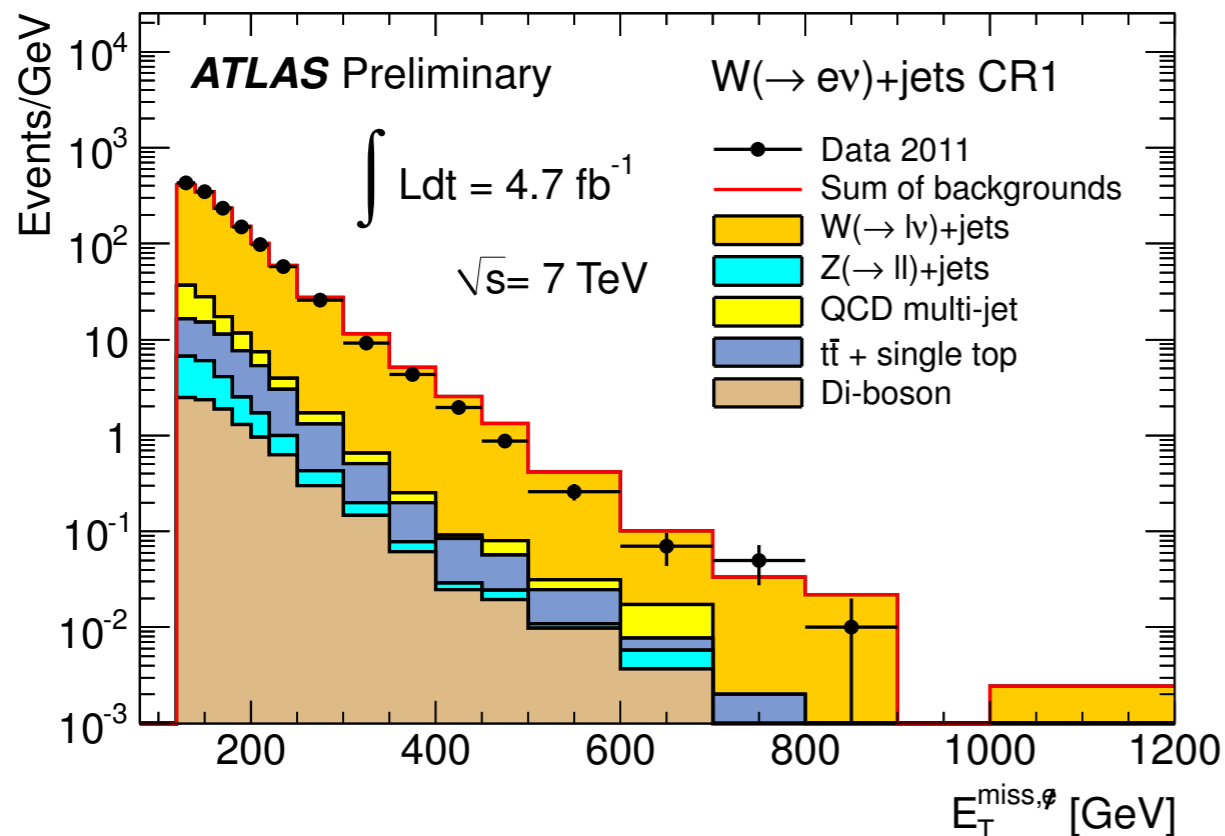


Sources of systematic uncertainties in the monojet analysis

Source	SR1	SR2	SR3	SR4
JES/JER/ E_T^{miss}	1.0	2.6	4.9	5.8
MC Z/W modelling	2.9	2.9	2.9	3.0
MC stat. uncert.	0.5	1.4	3.4	8.9
$1 - f_{EW}$	1.0	1.0	0.7	0.7
Muon scale and resolution	0.03	0.02	0.08	0.61
Lepton scale factors	0.4	0.5	0.6	0.7
Multijet BG in electron CR	0.1	0.1	0.3	0.6
Di-boson, top, multijet, non-collisions	0.8	0.7	1.1	0.3
Total systematic uncertainty	3.4	4.4	6.8	11.1
Total statistical uncertainty	0.5	1.7	4.3	11.8

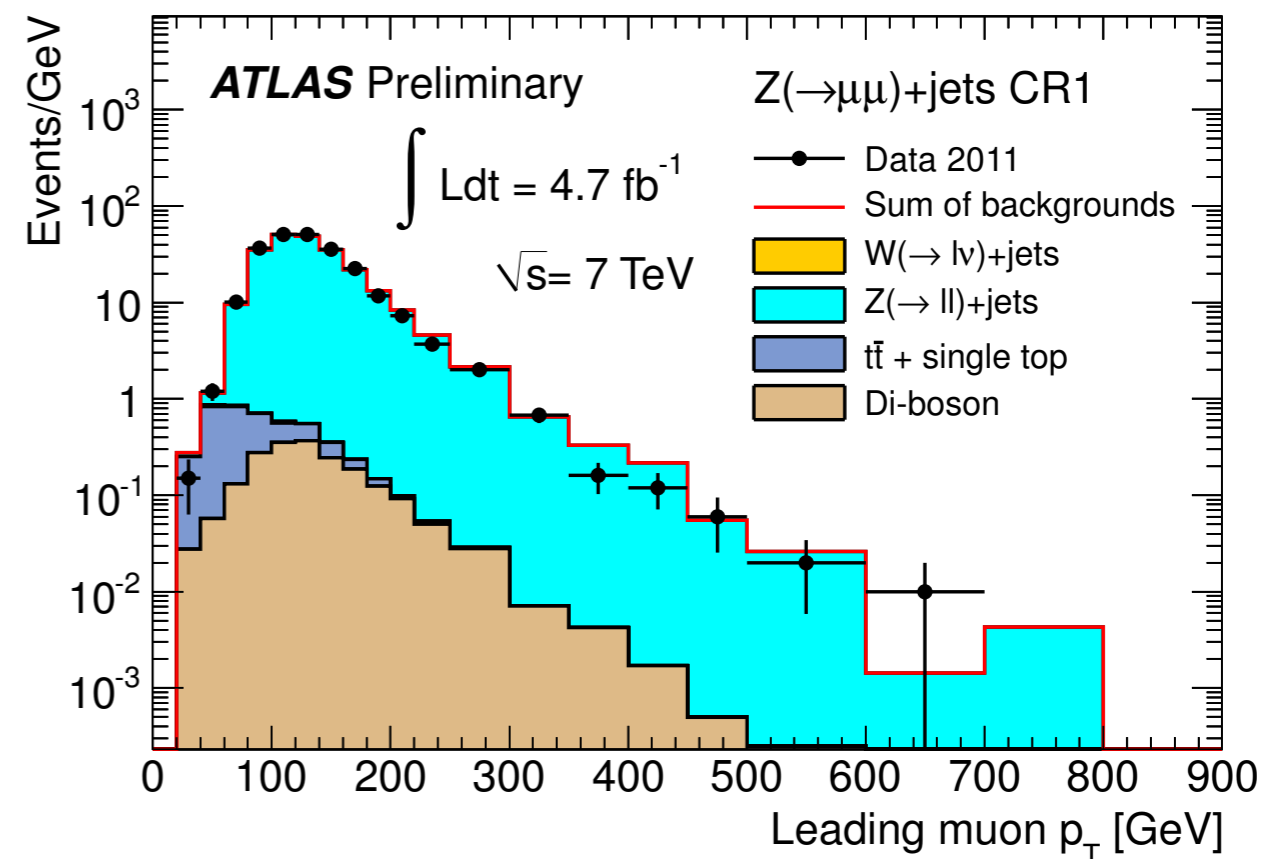
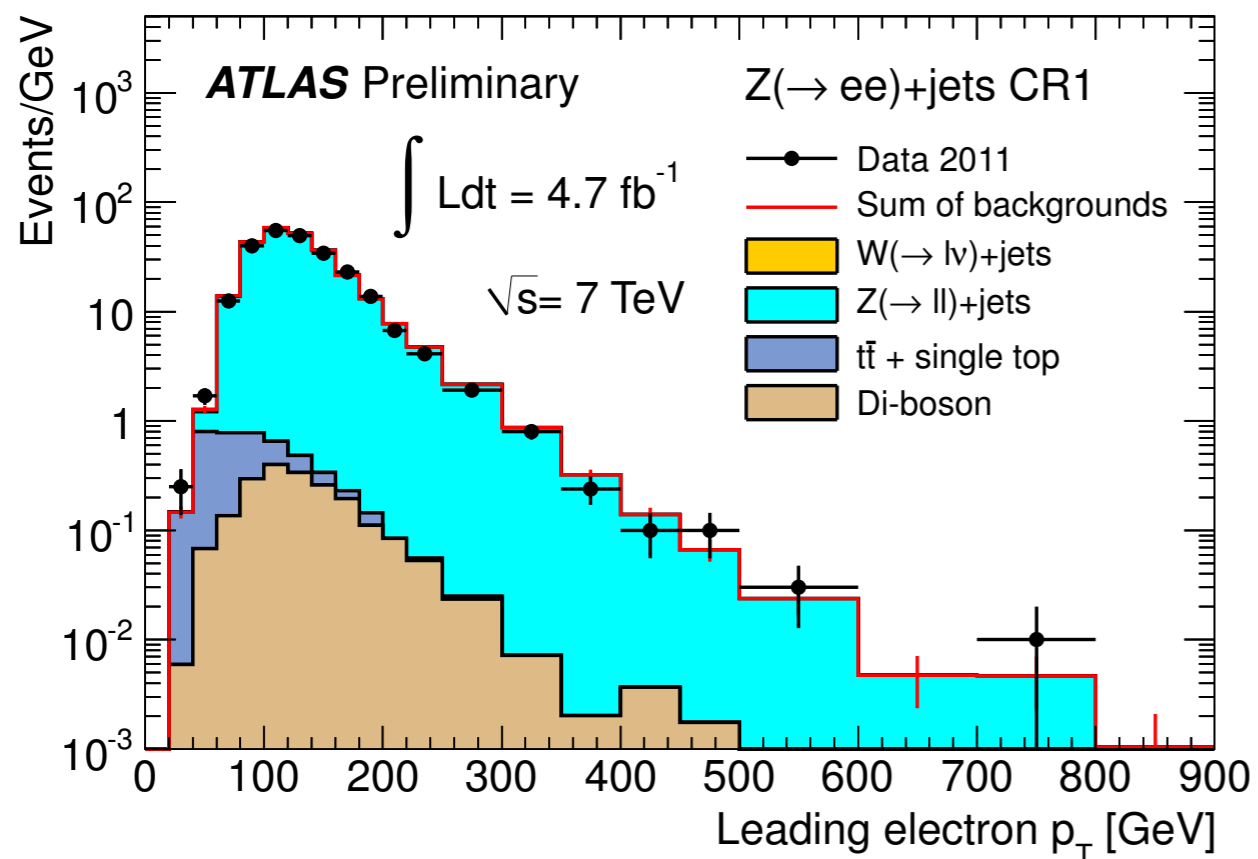
Muon Control Regions

- $Z \rightarrow \mu\mu$
 - MET trigger
 - exactly 2 muons
 - $66 < m_{\mu\mu} < 116$ GeV
- $W \rightarrow \mu\nu$
 - MET trigger
 - exactly 1 muon
 - MET (calo-muon) > 25 GeV
 - $m_T(l, \text{MET}) > 40$ GeV
- Otherwise, except for the lepton selection, all control regions use the same cuts as in the signal region selection.



Electron Control Regions

- $Z \rightarrow ee$
 - electron trigger
 - exactly 2 electrons
 - $66 < m_{ll} < 116$ GeV
- $W \rightarrow e\nu$
 - MET trigger
 - exactly 1 electron
 - MET (calo+electron) > 25 GeV
 - $40 < m_T(l, MET) < 100$ GeV
- Otherwise, except for the lepton selection, all control regions use the same cuts as in the signal region selection.



Example of beam background event

